

# Electronic structure and interaction in CH<sub>4</sub>@C<sub>60</sub> : A first-principle investigation

ang jia

Jinzhou Medical University

he huang

Jinzhou Medical University

zhong-fu zuo

Jinzhou Medical University

Yongjin Peng (✉ [hunterpyj2016@163.com](mailto:hunterpyj2016@163.com))

Jinzhou Medical University <https://orcid.org/0000-0003-4412-7305>

---

## Research Article

**Keywords:** C<sub>60</sub>, electronic structure, interaction, first principle

**Posted Date:** March 28th, 2022

**DOI:** <https://doi.org/10.21203/rs.3.rs-1436706/v1>

**License:** © ⓘ This work is licensed under a Creative Commons Attribution 4.0 International License.

[Read Full License](#)

---

# Abstract

$\text{CH}_4@C_{60}$  was the first example an organic molecule has been embedded in  $C_{60}$ , and by far the largest molecule.  $\text{CH}_4$  can rotate freely in the molecular cage, and the carbon skeleton structure of the  $C_{60}$  has no obvious deformation. The electronic structure of  $\text{CH}_4@C_{60}$  and interaction between  $C_{60}$  and  $\text{CH}_4$  were studied under quantum mechanical calculation method. The different reaction sites on C-C bonds in  $C_{60}$  and the weak Van der Waals interaction between  $\text{CH}_4$  and  $C_{60}$  were shown clearly. These results and the orbital interaction between  $\text{CH}_4$  and  $C_{60}$  were helpful for understanding and further application of this unique biggest organic molecule  $\text{CH}_4$  contained in  $C_{60}$  structure so far.

## 1. Introduction

$C_{60}$  is a carbon allotrope consisting of 60 C atoms in the shape of a soccer ball. Since  $C_{60}$  has a hollow molecular cavity, it is also envisaged to use  $C_{60}$  as a molecular cage and embed other small molecules in  $C_{60}$ . In theory, this process is simple: specific chemical means are used to cut the C-C bonds of several consecutive five-membered carbon rings and six-membered carbon rings on one side of the  $C_{60}$ , open a gap, introduce small molecules, and finally close the rings one by one by the same chemical method to suture the sphere.

In the past, small inorganic molecules such as  $\text{H}_2$ ,  $\text{H}_2\text{O}$  and  $\text{HF}$  have been embedded into  $C_{60}$ . [1–19] In order to plug larger molecules into the  $C_{60}$ , a larger gap has to be opened on its surface. However, over opening prevents further stitching of the  $C_{60}$ , thus limiting the size of the embedded molecules.

Professor Richard J. Whitby's team opened a large gap on one side of a  $C_{60}$  molecule, a 17-membered ring containing an S atom, and then tucked the  $\text{CH}_4$  into the cavity of  $C_{60}$  at high pressure. [20] The next step is the key suturing step, in which the sulfide in the gap is partially oxidized to sulfoxide, and desulfonation occurs under photoinitiation to complete the first closing, and then the structure of  $C_{60}$  is reduced by mature cyclization and aromatization processes. With the shielding of  $C_{60}$ , the quantum properties of C atom in a single  $\text{CH}_4$  molecule can be studied in this structure.

The stability and interaction in the structure of encapsulation of small molecules into fullerene nanocages have been studied by some previous theoretical work. [3, 6, 16, 21–24] Whereas the  $\text{CH}_4@C_{60}$  structure was probed using some new quantum mechanical calculation methods in this work and the interaction between  $C_{60}$  and  $\text{CH}_4$  was shown more clearly.

## 2. Theoretical Method

The wB97X-D3 exchange-correlation functional [25] in conjunction with def2-TZVP basis set [26] in vacuum were employed for geometric structure optimization and electronic structure calculation within the ORCA 4.2.1 code. [27] This combination of functional and basis set was shown to be reliable

especially for the quantum mechanical calculation of carbon materials.[28] All analyses were finished by using the Multiwfn 3.7 code[29] and some isosurface maps were rendered by means of VMD 1.9.3 software.[30]

The most stable optimized geometric structure of  $\text{CH}_4@C_{60}$  was obtained with the lowest energy and the number of the imaginary frequency of vibration was checked to be zero.

### 3. Results And Discussion

From the isosurface map of electron density in Fig. 1a, the symmetrical distribution of electron in  $\text{CH}_4@C_{60}$  was clearly shown. The electron density along the C-C bonds shared by one five-membered and one six-membered carbon ring ([5, 6] bond, labeled by 1 in Fig. 1) was smaller than C-C bonds shared by two six-membered carbon rings ([6, 6] bond, labeled by 2 in Fig. 1). This character was also clearly shown in isosurface map of gradient norm (Fig. 1b) and laplacian (Fig. 1c) of electron density.

The value of the laplacian function was defined as the trace of the electron density Hessian matrix at a point, which was the result of the Laplace operator applied to the electron density. The positive value of laplacian function means that the electron density was mainly divergent, otherwise the negative value mean that aggregation of electron density was dominant. In the isosurface map of laplacian of electron density of  $\text{CH}_4@C_{60}$  (Fig. 1c), the positive value was indicated by green color and the purple color was used to indicate negative value. It can be clearly seen that the positive laplacian value at the center of carbon and the negative laplacian value along the C-C bonds and the center of hydrogen atom which indicated the flow direction of the electron in this molecule. The symmetrical distribution of electron density and the difference between the [5, 6] and [6, 6] bonds were also clearly shown in isosurface map of laplacian of electron density (Fig. 1c).

To illustrate the interaction between  $\text{CH}_4$  and the  $C_{60}$  in detail, the  $\delta g$ [31] function of interaction area in the molecule were obtained through the multi wavefunction analysis software Multiwfn 3.7. It can be clearly shown that only the weak Van der Waals interaction of C-H... $\pi$  exist between the  $\text{CH}_4$  and  $C_{60}$  which was same as the results of experiments before.[20]

The distribution of molecular orbital of  $\text{CH}_4@C_{60}$  was illustrated by Density-of-states (DOS) map in Fig. 3. The DOS curve reflected the number of molecular orbitals in unit energy interval at corresponding energy. The total DOS (TDOS) of  $\text{CH}_4@C_{60}$  and the partial DOS (PDOS) of maps contributed by  $C_{60}$  and  $\text{CH}_4$  respectively were simultaneously shown in Figure. 3. Meanwhile isosurface maps of three molecular orbitals (orb92, HOMO, LUMO) with energy at about - 22.42eV, -8.10eV and - 2.12eV respectively at the current wB97XD3/def2-TZVP level were also drawn in the Figure for comparison. It can be seen from Fig. 3 that the HOMO and LUMO of the  $\text{CH}_4@C_{60}$  molecule were almost solely contributed by the  $C_{60}$  structure yet without the admixture of  $\text{CH}_4$  part. Within the occupied orbitals there were only several molecular orbitals with energy about - 23eV, -16eV and - 13eV in which the  $\text{CH}_4$  component made the contribution. This conclusion can also be deduced by the isosurface maps of molecular orbitals in Fig. 3.

The charge decomposition analysis (CDA) method was a valuable tool to analyze quantitatively the interactions between two molecular fragments in terms of the linear combination of the donor and acceptor fragment orbitals' donation and polarization using quantum mechanical calculations.[32] Within the  $\text{CH}_4@C_{60}$  molecule, the  $C_{60}$  and  $\text{CH}_4$  were defined as two fragments to be analyzed using CDA method. According to the results of CDA analysis, the orbital interaction between two fragments of  $C_{60}$  and  $\text{CH}_4$  were illustrated in Fig. 4. The solid and dashed horizontal bar in the Figure indicated the occupied and unoccupied molecular orbital respectively. The  $\text{CH}_4@C_{60}$  molecular orbital was connected by red line with the fragments' orbital which contributed more than 10% in that molecular orbital. It can be also seen in Fig. 4 that mostly the  $\text{CH}_4@C_{60}$  molecular orbitals including HOMO and LUMO were contributed by the  $C_{60}$  structure. The  $\text{CH}_4$  part just played a role in few occupied and unoccupied  $\text{CH}_4@C_{60}$  molecular orbitals which agreed with the conclusion from Fig. 3 mentioned before.

Fukui function and related dual descriptors are very popular methods defined under the framework of conceptual density functional theory for predicting reaction sites. Fukui functions and related dual descriptors are fine for most systems. However, for some systems which have higher order point group symmetry (tends to degenerate the frontline molecular orbitals) the Fukui function and the dual descriptor may give meaningless results, such as the distribution of the function does not satisfy the symmetry of the system, and therefore obviously violates the basic chemical intuition. Ricardo et al put forward the concept of orbital weighted Fukui function and dual descriptor of orbital weighted.[33, 34] Compared with the general form of Fukui function and double descriptors, the orbital weighted form has the advantage that it can be reasonably applied to the system of line orbital (quasi) degeneration, and for the system with symmetry, the results completely satisfy the molecular symmetrical structure.

Here the orbital weighted double descriptors of  $\text{CH}_4@C_{60}$  obtained from Multiwfn were illustrated in Fig. 5 to present the reaction sites of the molecule.

The negative value of orbital weighted double descriptors on [6, 6] bond (purple) indicated it was most easily electrophilic attacked. Otherwise, the positive value of orbital weighted double descriptors on [5, 6] bond (green) indicated it was most easily nucleophilic attacked. This result was similar as the former study on  $C_{60}$  and reflected the weak interaction between  $\text{CH}_4$  and  $C_{60}$ . To further understand the vibrational properties of  $\text{CH}_4@C_{60}$ , the IR spectrum was calculated and displayed in Fig. 6. The several obvious peaks came from the vibration modes of  $C_{60}$  part which indicated the negligible interaction between  $C_{60}$  and  $\text{CH}_4$  at this energy level.

## 4. Conclusion

In summary, the electronic structure and interaction between fragments inside the  $\text{CH}_4@C_{60}$  molecule were studied using quantum chemical method based on density functional theory. The different reaction sites on [5, 6] and [6, 6] bonds and the weak Van der Waals interaction between  $\text{CH}_4$  and  $C_{60}$  were shown clearly. The calculated IR spectrum indicated the negligible interaction between  $C_{60}$  and  $\text{CH}_4$  at the

vibrational energy level. These results and the orbital interaction between CH<sub>4</sub> and C<sub>60</sub> were helpful for understanding and further application of this unique biggest organic molecule CH<sub>4</sub> contained in C<sub>60</sub> structure so far.

## Declarations

### Acknowledgement

This work was supported by the Natural Science Foundation of Liaoning Province (JYTQN201923, 20180550512), National Natural Science Foundation of China (81374051)

### Conflicts of interest/Competing interests

No conflict to declare.

### Availability of data and material

All the data can be shared in the supporting information online.

### Code availability

The software ORCA and VMD used in this work can be downloaded freely.

### Authors' contributions

Jia ang performed the calculation; Huang he and Zuo zhong-fu performed the data analysis; peng yong-jin designed and analyzed the data.

## References

1. Wakahara T, Kato T, Miyazawa Ki, Harneit W (2012) N@C-60 as a structural probe for fullerene nanomaterials. *Carbon* 50:1709–1712
2. Yang J, Feng P, Sygula A, Harneit W, Su J-H, Du J (2012) Probing the zero-field splitting in the ordered N@C-60 in buckycatcher C60H28 studied by EPR spectroscopy. *Phys Lett A* 376:1748–1751
3. Huang J, Li Q, Yang J (2013) Tuning the Electronic Properties of N@C-60 Molecule: A Theoretical Study. *J Nanosci Nanotechnol* 13:1053–1058
4. Liu G, Gimenez-Lopez MdC, JeVric M, Khlobystov AN, Briggs GAD, Porfyrakis K (2013) Alignment of N@C-60 Derivatives in a Liquid Crystal Matrix. *J Phys Chem B* 117:5925–5931
5. Min K, Farimani AB, Aluru NR (2013) Mechanical behavior of water filled C60, *Appl. Phys. Lett.*, 103
6. Yu Z, Chen J, Zhang L, Wang J (2013) First-principles investigation of quantum transport through an endohedral N@C-60 in the Coulomb blockade regime, *Journal Of Physics-Condensed Matter*, 25

7. Plant SR, Porfyrakis K (2014) Using electron paramagnetic resonance to map N@C-60 during high throughput processing. *Analyst* 139:4519–4524
8. Eckardt M, Wieczorek R, Harneit W (2015) Stability of C-60 and N@C-60 under thermal and optical exposure. *Carbon* 95:601–607
9. Li G (2015) Tuning conductance in C-60 deVices: defective C-60 and endohedral C-60 complex, vol 118. *Applied Physics a-Materials Science & Processing*, pp 473–477
10. Min K, Farimani AB, Aluru NR (2015) Mechanically modulated electronic properties of water-filled fullerenes. *MRS Commun* 5:305–310
11. Sabirov DS, Tukhbatullina AA, Bulgakov RG (2015) Compression of Methane Endofullerene CH<sub>4</sub>@C-60 as a Potential Route to Endohedral Covalent Fullerene Derivatives: A DFT Study, *Fullerenes Nanotubes And Carbon Nanostructures*, 23835–842
12. Zhou S, Rasovic I, Briggs GAD, Porfyrakis K (2015) Synthesis of the first completely spin-compatible N@C-60 cyclopropane derivatives by carefully tuning the DBU base catalyst. *Chem Commun* 51:7096–7099
13. Cornes SP, Zhou S, Porfyrakis K (2017) Synthesis and EPR studies of the first water-soluble N@C-60 derivative. *Chem Commun* 53:12742–12745
14. Zhao Y, Wang B (2018) Effect of Substrate on the Electron Spin Resonance Spectra of N@C-60 Molecules. *Acta Phys Chim Sin* 34:1312–1320
15. Hashikawa Y, Murata Y (2019) H<sub>2</sub>O/Olefinic- $\pi$  Interaction inside a Carbon Nanocage. *J Am Chem Soc* 141:12928–12938
16. Xu M, Felker PM, Mamone S, Horsewill AJ, Rols S, Whitby RJ, Bacic Z, Breaking S (2019) *J. Phys. Chem. Lett.*, 10 5365–5371
17. Bloodworth S, Hoffman G, Walkey MC, Bacanu GR, Herniman JM, LeVitt MH, Whitby RJ (2020) Synthesis of Ar@C(60) using molecular surgery. *Chem Commun* 56:10521–10524
18. Felker PM, Bacic Z (2020) Flexible water molecule in C-60: Intramolecular vibrational frequencies and translation-rotation eigenstates from fully coupled nine-dimensional quantum calculations with small basis sets, *J. Chem. Phys.*, 152
19. Kurotobi K, Murata, Yasujiro AS (2011) Molecule of Water Encapsulated in Fullerene C<sub>60</sub>, *Science*,
20. Bloodworth S, Sotinova G, Alom S, Vidal S, Bacanu GR, Elliott SJ, Light ME, Herniman JM, Langley GJ, LeVitt MH, Whitby RJ (2019) First Synthesis and Characterization of CH<sub>4</sub>@C-60. *Angewandte Chemie-International Edition* 58:5038–5043
21. Cong W, Michal, Straka, Pekka, Pyykk? (2010) Formulations of the closed-shell interactions in endohedral systems. *PCCP, Physical chemistry chemical physics*
22. Korona T, Dodziuk H (2011) Small Molecules in C<sub>60</sub> and C<sub>70</sub>: Which Complexes Could Be Stabilized? *J Chem Theory Comput* 7:1476
23. Popov AA, Yang S, Dunsch L, Fullerenes E (2013) *Chem ReV* 113:5989–6113

24. Zeinalinezhad A, Sahnoun R (2020) Encapsulation of Hydrogen Molecules in C<sub>50</sub> Fullerene: An ab Initio Study of Structural, Energetic, and Electronic Properties of H<sub>2</sub>@C<sub>50</sub> and 2H<sub>2</sub>@C<sub>50</sub> Complexes. ACS Omega 5:12853–12864
25. Grimme S, Ehrlich S, Goerigk L (2011) Effect of the damping function in dispersion corrected density functional theory. J Comput Chem 32:1456–1465
26. Weigend F, Ahlrichs R (2005) Balanced basis sets of split valence, triple zeta valence and quadruple zeta valence quality for H to Rn: Design and assessment of accuracy. PCCP 7:3297–3305
27. Neese F (2018) Software update: the ORCA program system, version 4.0, vol 8. Wiley Interdisciplinary ReViews Computational Molecular ence, p e1327
28. Liu Z, Lu T, Chen Q (2020) An sp-hybridized all-carboatomic ring, cyclo[18]carbon: Electronic structure, electronic spectrum, and optical nonlinearity. Carbon 165:461–467
29. Lu T, Chen F, Multiwfn (2012) A multifunctional wavefunction analyzer. J Comput Chem 33:580–592
30. Humphrey W, Dalke A, Schulten K (1996) Visual molecular dynamics. J Mol Graph 14:33–38
31. Lefebvre C, Rubez G, Khartabil H, Boisson JC, Contrerasgarcía J, Hénon E (2017) Accurately extracting the signature of intermolecular interactions present in the NCI plot of the reduced density gradient versus electron density. PCCP, p 19
32. Dapprich S, Frenking G (1995) Investigation of Donor-Acceptor Interactions: A Charge Decomposition Analysis Using Fragment Molecular Orbitals. J Phys Chem 99:9352–9362
33. Ruiz L (2017) Tiznado, William, Cardenas, Carlos, Inostroza, Diego, Pino-Rios, Ricardo, Proposal of a Simple and Effective Local Reactivity Descriptor through a Topological Analysis of an Orbital-Weighted Fukui Function, Journal of Computational Chemistry Organic Inorganic Physical Biological,
34. Pino-Rios R, Inostroza D, Cardenas-Jiron G, Tiznado W (2019) Orbital-Weighted Dual Descriptor for the Study of Local Reactivity of Systems with (Quasi-) Degenerate States. J Phys Chem A 123:10556–10562

## Figures

### Figure 1

CH<sub>4</sub>@C<sub>60</sub> isosurface maps of (a) electron density, value=0.25 (b) gradient norm of electron density, value=0.25 (c) laplacian of electron density, value=±0.7

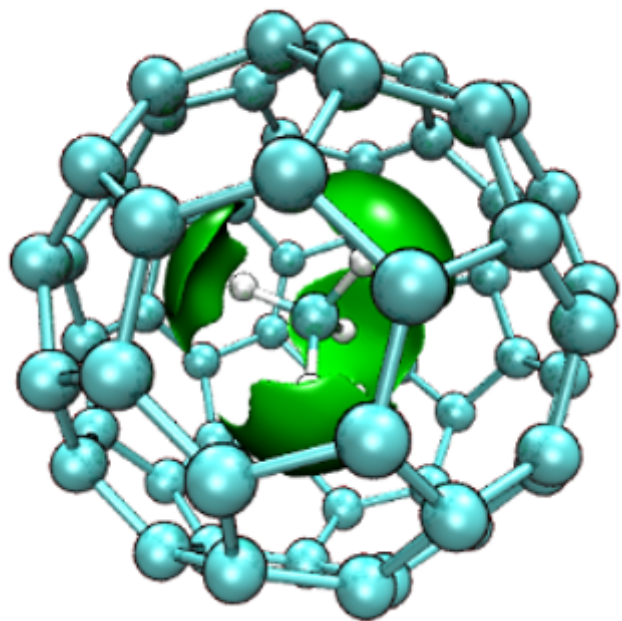
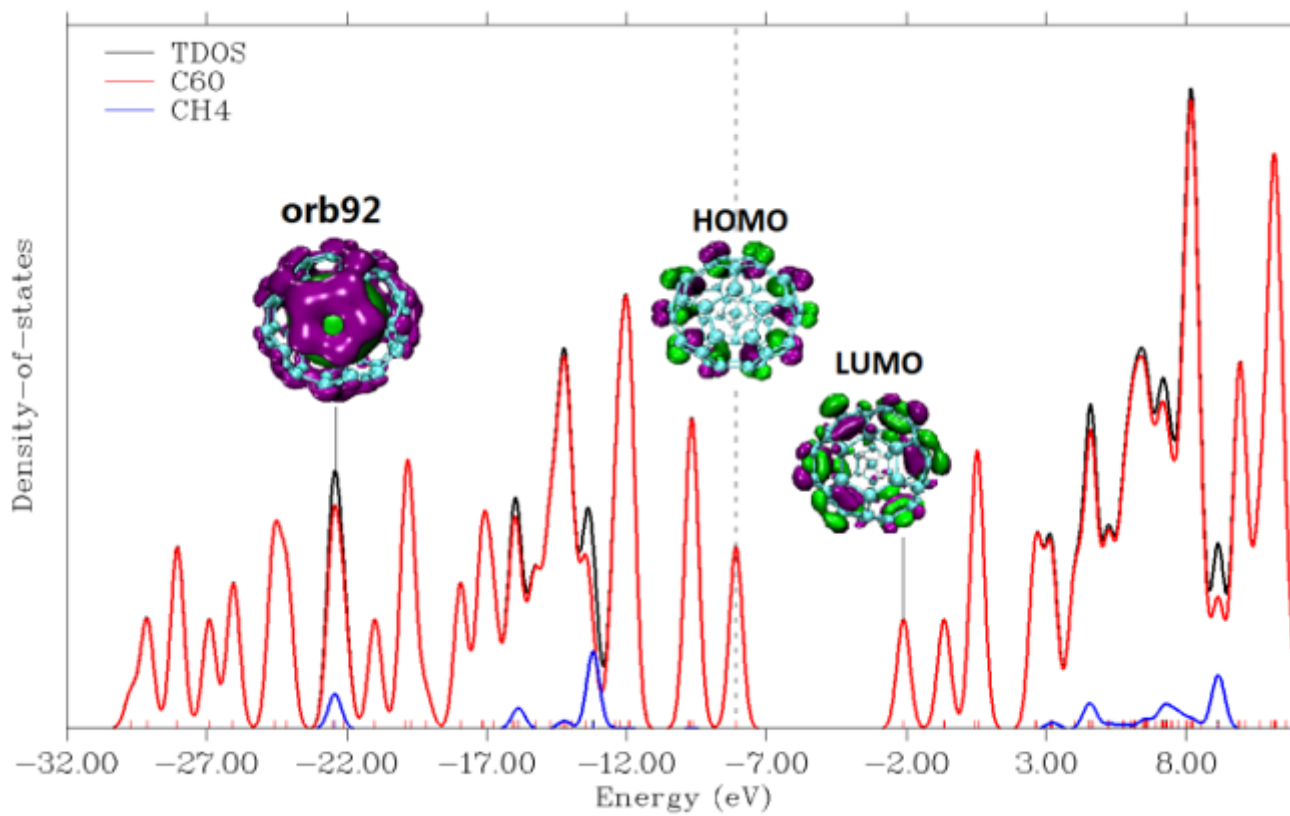


Figure 2

$\delta g$  function of interaction area in  $\text{CH}_4@C_{60}$



**Figure 3**

The total DOS (TDOS) of  $\text{CH}_4@C_{60}$  and the partial DOS (PDOS) of maps contributed by  $C_{60}$  and  $\text{CH}_4$  respectively (value for isosurface map=  $\pm 0.004$ )

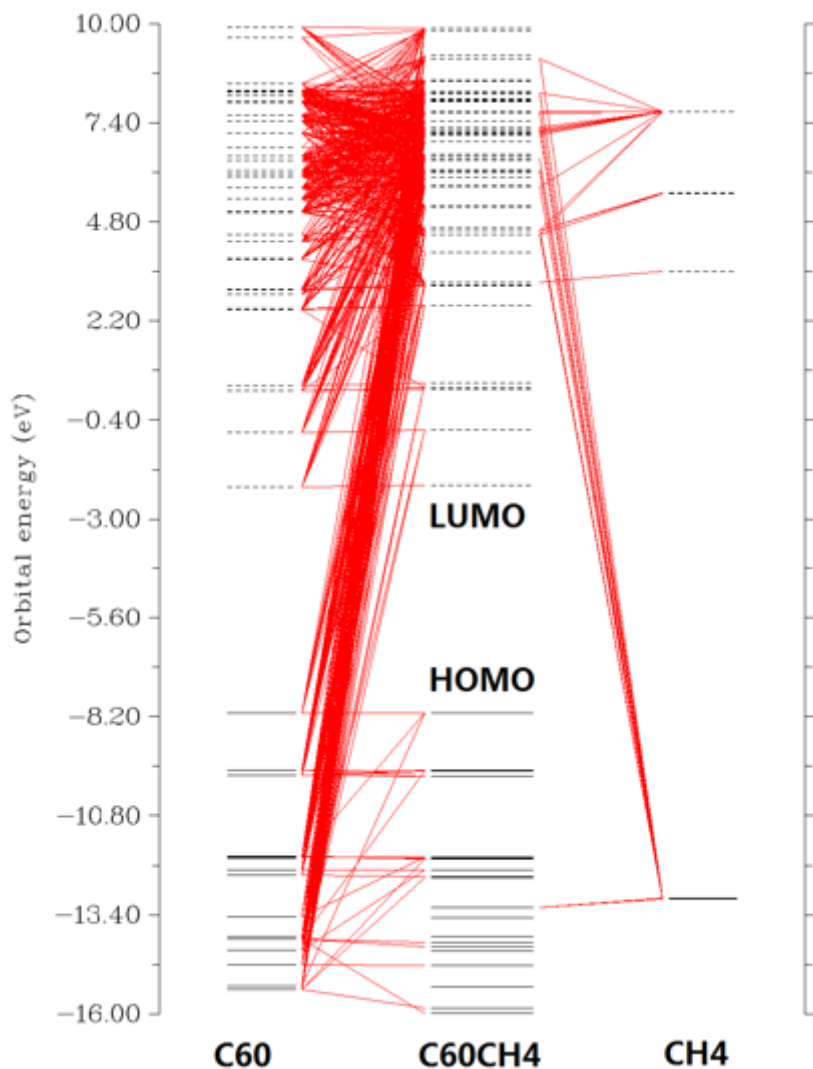


**Figure 4**

The orbital interaction between two fragments of  $C_{60}$  and  $\text{CH}_4$

**Figure 5**

The isosurface maps of orbital weighted double descriptors of  $\text{CH}_4@C_{60}$  (value= $\pm 0.001$ )

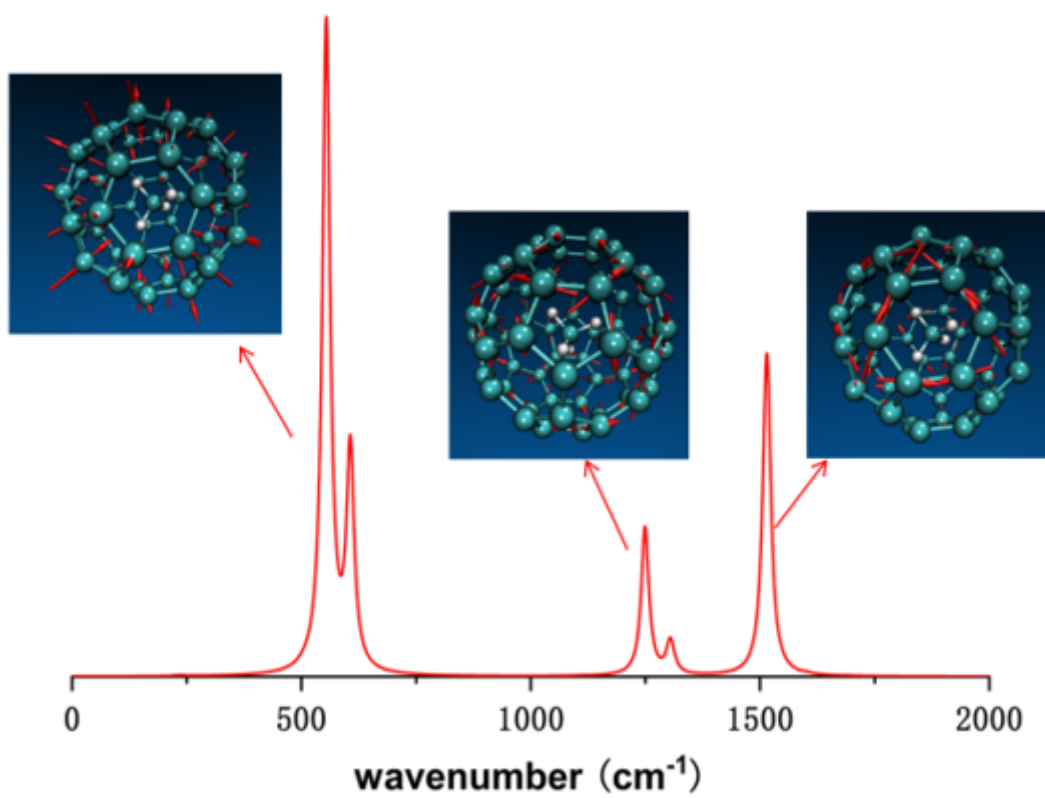


Figure 6

the calculated IR spectrum of CH<sub>4</sub>@C<sub>60</sub>